Journal of Advanced Research in Fluid Mechanics and Thermal Sciences

Journal homepage:
https://semarakilmu.com.my/journals/index.php/fluid_mechanics_thermal_sciences/index
ISSN: 2289-7879

Analysis of Energy and Mass Transport Flow of Ethyleneglycol ($C_2H_6O_2$) Based Nanofluid over an Infinite Porous Plate

Mummadisetty Umamaheswar[1], Peram Madhu Mohan Reddy[2], Obulesu Mopuri[2], Anumula Vidhyullatha[3], Nakkarasupalli Mallikarjuna Reddy[4], Ankita Tiwari[5], Charan Kumar Ganteda[5,*], Koppula Rama Thulasi[6]

[1] Department of Mathematics, Annamacharya Institute of Technology and Sciences (Autonomous), Rajampet-516126, A.P., India
[2] Department of Mathematics, Siddharth Institute of Engineering &Technology (Autonomous), Puttur-517583, A.P., India
[3] Department of Mathematics, SPW Degree & PG College, TTD, Tirupati-517502, A.P., India
[4] Department of Mathematics, RJS First Grade College, Koramangla, Bengaluru-560034, Karnataka, India
[5] Department of Engineering Mathematics, College of Engineering, Koneru Lakshmaiah Education Foundation, Vaddeswaram 522301, Andhra Pradesh, India
[6] Department of Mathematics, Malla Reddy Engineering College (Autonomous), Hyderabad, India

ARTICLE INFO

Article history:
Received 28 April 2023
Received in revised form 12 July 2023
Accepted 19 July 2023
Available online 6 August 2023

Keywords:
MHD; nanofluid; radiation absorption; Dufour effect; porous medium; chemical reaction

ABSTRACT

The main aim of this article is to analyze the flow properties of energy and mass transport flow of ethylene glycol ($C_2H_6O_2$) based nanofluid over an infinite porous plate. A constant velocity U0 is applied to the plate, and warmth and attention are unspecified to fluctuate harmonically as of a steady denote at the shield through occasion. Three kinds of fluid nanoparticles namely Cu-$C_2H_6O_2$, CuO-$C_2H_6O_2$ as well as TiO_2-$C_2H_6O_2$ nano fluids are used. Through graphs and tables, the impacts of different fluid flow parameters are examined. The new parameters added in this analysis are thermal radiation and the angle of inclination. The objective of this work is to derive exact solution by perturbation method and analyze the variations in the flow. The diffusion thermo parameter as well as the radiation absorption parameter have been observed to improve the speed, the hotness, plus the resistance between skin cells. An examination of the skin friction coefficient numerically in detail for the engineering industry. This development has main consequences for Particles of nanoscale. The solid particles have an elevated conductivity, which accounts for this of Cu, CuO than those of TiO_2. In addition, by means of an augment in the substance response constraint, it is seen so as to the solutal border layer thickness decreases.

1.Introduction

Recently, attention has been drawn to mesoscopic approaches. The primary heat transmission method in many applications is free convection. Because of its many uses in businesses, electronics, solar energy, and the cooling of electrical and mechanical components, convection has an essential place in nature and engineering. Nanofluid may be suggested as a practical means of enhancing

[*] *Corresponding author.*
E-mail address: charankumargnteda@kluniversity.in

https://doi.org/10.37934/arfmts.108.1.136157

heat transfer. The transport process is now being improved by scientists and engineers in various engineering systems, such as heat exchanges, electrical strategy, substance reactors, in addition to others. It is feasible to alter various system components being studied for this purpose, such as temperature transport surfaces or operation all liquid. As a grouping of graceful liquid and Particles of nano size of hard substance, nanofluids (Nfs) can be regarded as useful operational liquids that can be used in a variety of engineering systems. It has been extensively explored how nanofluids can enhance thermal, electrical, and power electronics' warmth relocate capabilities. Water, ethylene glycol, as well as mineral oil are heat transfer in conventional cooling systems. Coolants such as nanofluids (Nfs) have a better thermal conductivity and cooling performance than conventional coolants. A major reason for nanofluids' popularity is their ability to transfer heat. Because nanofluids are being used in real time, researchers are constantly seeking to understand the properties of these nanofluids. Researchers are drawn to nanofluid applications because they inform their study uses in accordance with the present social concerns. Ali and Salam [1] have specified a review on some of the properties as well as uses of Nanofluids in various sectors of society. Such as defence, solar desalination, oil transformers, refrigeration etc. Eastman *et al.,* [2] have compared their thoughts of nanofluids with Hamilton–Crosser theory [3]. Recent technological advances in machine learning and artificial intelligence have endeavour by Sharma *et al.,* [4] to present their views with an emphasis on the implementations of nanofluids in these fields. Jama *et al.,* [5] have investigated on diverse nanofluids with different base fluids and demonstrated some of these applications like biomedical applications, automotive cooling, magnetic sealing, nanofluid detergent etc. Experiments conducted by Kleinstreuer and Feng [6] recommended using a variety of measurement strategies in arrange to determine the thermal conductivity of Fluids with nanostructures. Several projected models for determining the nanofluids' thermal efficiency have been explored by Junhao *et al.,* [7]. The run of a hybrid fluids of nanoscale through a shrinking riga shield was the topic of discussion between Nur *et al.,* [8]. Malvandi *et al.,* [9] incorporated three nanoparticles to transfer the heat over a blowing /suction as a boundary value problem.

Bhattacharyya*et al.,* [10] taken a look at the implications of partial slip-on laminar pour, by considering the occurrence of dual solutions and solving the problem from a mathematical standpoint. Emed and Pop [11] conveyed some of the variations among nanofluids and hybrid nanofluids. They also analyzed the behaviour of these fluids and found that there were three distinct regions of stability. Sajad *et al.,* [12] discussed about hybrid fluids of nanoscaleby means of a mixing of water and Ethylene-glycol with different hybrid particles of nanoscale. They have solved the problem by Akbari- Ganji's method and compared with the numerical explanation. Manohar *et al.,* [13] established hybrid carbon nanotubes problem solved with the maple program with three various base fluids and analyzed in depth. Javali *et al.,* [14] have investigated about sinusoidal radius activity in the flow of hybrid fluids with nanostructures. Muhaimin *et al.,* [15] concentrated on CNT nanofluids with thermal stratification by observing the thermo physical properties at SWCNT as well as MWCNT. Physical parameters were compared on MHD flows with hall current effects Das *et al.,* [16] using Laplace technique. Chandra Shekar *et al.,* [17] have put more interest on the study of nanofluids past a porous square cavity. Adnan *et al.,* [18] have completedanarithmeticalexamination on the nanodiamond materials. Dave *et al.,* [19] discussed about graphene nano fluids with dust particles.

It is generally believed that liquid such as water, different types of oils, in addition to ethylene glycol contain a small thermal efficiency, which is the major obstacle to increasing heat transfer rates beyond a certain point. Many authors have suggested that wavy geometries and/or metal nano particles can solve this problem. As an innovative project, Choi *et al.,* To improve thermal

conductivity, they added solid components of nano size (less than 100 nm in diameter) into the base fluid. Nanoliquid when compared with micrometre and millimetre-sized particles, nano liquids possess single substance with corporeal properties such as reduced pumping power, high stability with low sedimentation, and high thermal conductivity without clogging microchannels [20]. Nanofluids (Nfs) are used in a variety of industrial processes, including heat exchange, lubrication, and microchannel heat sinks. Since forced convection flows inside of channels are widely used in industry, increasing the thermal energy transmission coefficient has long been a source of frustration among heat transfer (HT) experts. Veera Krishna *et al.,* [21] study of the Casson hybrid nano fluid's radiative MHD flow over an infinitely fast vertical porous surface. Suspending tiny solid particles in the fluids is an inventive method of enhancing the heat transfer of fluids. In 1995, the term "Nanofluid" was first used to describe this new type of fluid by Choi. a variety of applications in contemporary A wide range of science, technology, and engineering fields, including chemical manufacturing, automobile manufacturing, solar collectors, nuclear reactors, industrial cooling, and gas sensing, etc. There are several ways to improve the warmthrelocate of prepared solutions, single of which is to hang up. Microparticles (Cu, CuO, Ag, Au, MgO, Al_2O_2, TiO_2, etc.) with sizes stuck between 1 and 100 nm in the base liquid (such as water, $C_2H_6O_2$ (ethylene-glycol), glycerine, or blood $C_2H_8O_6$) (sodium alginate). The idea is to enhance the beneficial thermal properties of microparticles and avoid. Hayat *et al.,* [22] the temperature profile decreases as the thermal and slip stratification parameters are increased, according to an analysis of MHD nano fluid flow under double stratification and slip conditions. The activation energy in a reactive system is a crucial energy required for chemical species atoms or molecules to initiate a reaction. Khan *et al.,*[23]alumina with hydro magnetic dissipation was studied A moving wedge is passed by a nanofluid. In the energy equation, they included the impact of thermal radiation. Hayat *et al.,* [24] examined the effect of radiation warmthrelocate in a container. Sheikholeslami and Seyednezhad [25] simulated effects of an excitingmeadow on particles of nano sizegratis convection in a permeable medium.

Many industrial, scientific, and engineering applications have recently focused on the magnetohydrodynamic boarder line sheet pour of nano liquid plus warmth transport. Because nanometer-sized materials through single substance plus bodily properties contain numerous applications in industries, including electronics cooling plus transformer cooling, nano fluids are widely used. This study is particularly relevant to boilingundulating, dissolverotating, extrusion, glass threadmanufacture, wire drawing, manufacturing of artificialplus rubber sheets, as well as polymer sheets and filaments. Many researchers contributed to this field of study, including Venkateswara Raju *et al.,* and many researchers [26-31] researched the aforementioned uses of nano fluids, a computational analysis of nanofluid MHD marangoni convection pour by means of warmth plus accumulation transport characteristics across an absorbent media. Ahmed Zeeshan *et al.,* [32] deliberated energy analysis of non-Newtonian nanofluid flow over parabola of revolution on the horizontal surface with catalytic chemical reaction. Salahuddin *et al.,* [33] analysed Variable thermo physical characteristics of Carreau fluid flow by means of stretchable paraboloid surface with activation energy and heat generation.Salahuddin *et al.,* [33] considered Variable thermo physical characteristics of Carreau fluid flow by means of stretchable paraboloid surface with activation energy and heat generation.Salahuddin and Muhammad Awais [34] examined a comparative study of Cross and Carreau fluid models having variable fluid characteristics. Salahuddin *et al.,* [35] detected the impact of Soret and Dufour on permeable flow analysis of Carreau fluid near thermally radiated cylinder. Salahuddin *et al.,* [36] examined A permeable squeezed flow analysis of Maxwell fluid near a sensor surface with radiation and chemical reaction. Salahuddin *et al.,* [37] studied a noteworthy impact of heat and mass transpiration near the

unsteady rare stagnation region. Salahuddin *et al.,* [38] analysed a flow behaviour of Sutterby nanofluid near the catalytic parabolic surface. Salahuddin *et al.,* [39] studied Analysis of transport phenomenon in cross fluid using Cattaneo-Christov theory for heat and mass fluxes with variable viscosity.

Keeping the above-mentioned facts, a distinct kind of synthetic fluid known as the Nanofluids contains nanoparticles.We are encouraged to employ nanofluids as a coolant instead of regular liquids because of their increased thermal conductivity and improved heat transmission capacities.The analysis of energy and mass transport in a $C_2H_6O_2$-based nanofluid flowing freely in excess ofacountlessabsorbentshield has been described.In this manuscript, we explore the exact and closed form solutions to the poweras well asaccumulationtransfer analysis of a free ventilationpour of a $C_2H_6O_2$ nanofluid over anever-endingabsorbentshield. Perturbation is used to obtain speed, hotness, plus attentiveness solutions. In this analysis, the new parameters added to the published literature of Durga Prasad *et al.,* [31] are thermal radiation and the angle of inclination.This novelty is taken based on the importance of these results in petroleum industries.

2. Formulation of the Problem

Regard as an uneven two-dimensional, free convectional warmth plus accumulation transport pour of the ability to conduct electricity Hydrophobic nanofluids past a semi-infinite affecting permeable wall entrenched a uniform absorbentintermediate. The physical model a co-ordinates classification is show in Figure 1.

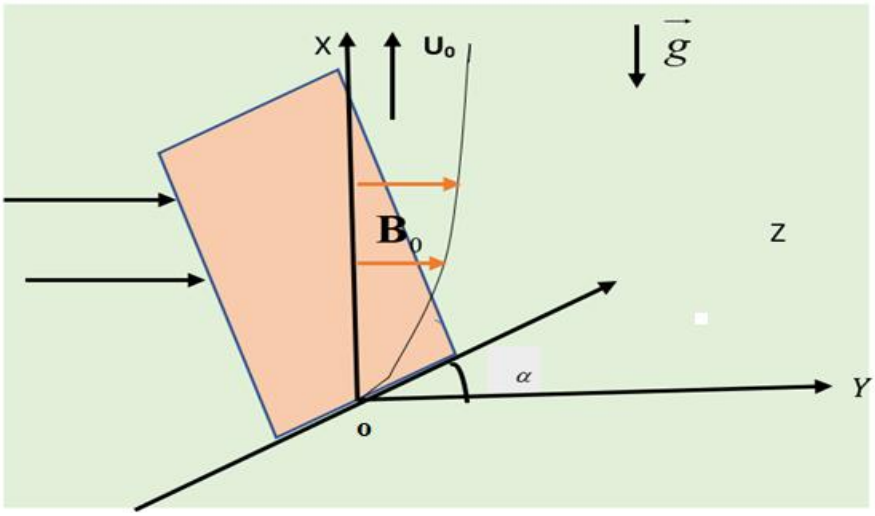

Fig. 1. Schematic drawing of the physical model

The flow is assumed to the χ-direction which is taken along the plate and γ- axis is normal to it. The plate inclined at an angle γ with the vertical and a uniform magnetic field of strength B_0 is applied in the direction which makes an angle α with the positive χ-axis. Diffusion thermo, Thermal radiation, constant heat source, Radiation absorption and first order Chemical reaction effects are considered.

2.1 Basic Governing Equations

The basic equations are used which result from the conservation of mass (The continuity equation), conservation of momentum (Navier-Stokes equation), conservation of energy (Energy equation) and conservation of concentration (Diffusion equation) in the following form.

$$\nabla.\bar{q} = 0 \tag{1}$$

$$\rho\left[\frac{\partial \bar{q}}{\partial t} + \bar{q}.\nabla\bar{q}\right] = \rho\bar{X} - \nabla p + \mu\nabla^2\bar{q} \tag{2}$$

$$\rho C_p \frac{\partial T}{\partial t} = \kappa\nabla^2 T \tag{3}$$

$$\frac{\partial C}{\partial t} = D\nabla^2 C \tag{4}$$

whereas the velocity vector, ρ is the density of the fluid near the plate, p is the pressure, μ is the coefficient of viscosity, C_p is the specific heat at constant pressure, T is the temperature of the fluid near the plate, *k* is the thermal conductivity of the fluid, q_r is the radiative heat flux, C is the species concentration in the fluid near the plate and D is the species diffusion coefficient.

In the present analysis, it is assumed that:

i. The absorbent wall is extendedsufficient in X'-direction in order that the pouruneven are function of y' and t'.
ii. Applied on electrical field and induced magnetic field are neglected.
iii. Initially the plate and the field are at the same temperature T_∞' and C_∞'.
iv. When $T' \geq 0$, the temperature and concentration at the plate are fluctuating with time.
v. The fluid is $C_2H_6O_2$ based nanofluid containing three types of nanoparticles are Cu, Cuo and TiO_2.
vi. The nanoparticles have uniform shape and size.
vii. Both the fluid phase and nanoparticles are in the thermal equilibrium state.

Under the above boundary layer approximation, the governing equations for the nanofluid flow are given by

2.1.1 Continuity equation

$$\frac{\partial u'}{\partial x'} + \frac{\partial v'}{\partial y'} = 0 \tag{5}$$

2.1.2 Momentum equation

$$\rho_{nf}\left(\frac{\partial u^{'}}{\partial t^{'}}+v^{'}\frac{\partial u^{'}}{\partial y^{'}}\right)=\mu_{nf}\frac{\partial^2 u^{'}}{\partial y^{'2}}+\left(\rho\beta\right)_{nf}g\cos\gamma\left(T^{'}-T_{\infty}^{'}\right)-\frac{\mu_{nf}u^{'}}{K^{'}}-\sigma{B_0}^2\sin^2\alpha u^{'} \tag{6}$$

2.1.3 Energy equation

$$\frac{\partial T^{'}}{\partial t^{'}}+v^{'}\frac{\partial T^{'}}{\partial y^{'}}=\alpha_{nf}\frac{\partial^2 T^{'}}{\partial y^{'2}}-\frac{Q^{'}}{\left(\rho C_P\right)_{nf}}(T^{'}-T_{\infty}^{'})+Q_l^{'}\left(C^{'}-C_{\infty}^{'}\right)+\frac{D_m K_T}{C_s(\rho C_p)_{nf}}\frac{\partial^2 C^{'}}{\partial y^{'2}}-\frac{1}{\left(\rho C_p\right)_{nf}}\frac{\partial q_r}{\partial y^{'}} \tag{7}$$

2.1.4 Species equation

$$\frac{\partial C^{'}}{\partial t^{'}}+v^{'}\frac{\partial C^{'}}{\partial y^{'}}=D_B\frac{\partial^2 C^{'}}{\partial y^{'2}}-K_1\left(C^{'}-C_{\infty}^{'}\right) \tag{8}$$

Suctionrestrictionstandard to the shield is, $v=-V_0$ (constant), where v is self-governing of y. As ofcorporealexplanation the governing Eq. (9) to Eq. (12) becomes,

$$\frac{\partial v^{'}}{\partial y^{'}}=0 \tag{9}$$

$$\rho_{nf}\left(\frac{\partial u^{'}}{\partial t^{'}}-V_0\frac{\partial u^{'}}{\partial y^{'}}\right)=\mu_{nf}\frac{\partial^2 u^{'}}{\partial y^{'2}}+\left(\rho\beta\right)_{nf}g\cos\gamma\left(T^{'}-T_{\infty}^{'}\right)-\frac{\mu_{nf}u^{'}}{K^{'}}-\sigma{B_0}^2\sin^2\alpha u^{'} \tag{10}$$

$$\frac{\partial T^{'}}{\partial t^{'}}-V_0\frac{\partial T^{'}}{\partial y^{'}}=\alpha_{nf}\frac{\partial^2 T^{'}}{\partial y^{'2}}-\frac{Q^{'}}{\left(\rho C_P\right)_{nf}}(T^{'}-T_{\infty}^{'})+Q_l^{'}\left(C^{'}-C_{\infty}^{'}\right)+\frac{D_m K_T}{C_s(\rho C_p)_{nf}}\frac{\partial^2 C^{'}}{\partial y^{'2}}-\frac{1}{\left(\rho C_p\right)_{nf}}\frac{\partial q_r}{\partial y^{'}} \tag{11}$$

$$\frac{\partial C^{'}}{\partial t^{'}}-V_0\frac{\partial C^{'}}{\partial y^{'}}=D_B\frac{\partial^2 C^{'}}{\partial y^{'2}}-K_1\left(C^{'}-C_{\infty}^{'}\right) \tag{12}$$

where $u^{'}$ and $v^{'}$ is the speedmechanism in χalong withγ- axis correspondingly. ρ_{nf} is the density of the liquid nanoscale, μ_{nf} is the stickiness of the fluid nanoparticles, β_{nf} is the coefficient of thermal elongation of fluid nanoscale, σ is A fluid's conductivity is determined by its electrical conductivity, and gravity's acceleration is determined by its acceleration, $\left(\rho C_p\right)_{nf}$ is the temperature capacitance of the nanofluid, $K^{'}$ is the permeability permeable intermediate, $T^{'}$ is the temperature of the nanofluid, Q is the rate at which a heat source produces volumetric heat in response to temperature, α_{nf} is the thermal diffusivity of the nanofluid. φ is the solid volume fraction of the fluid nanoparticles, K_{nf} and K_s are thermal conductivities of the base liquid plus solid, q_r is the radiative warmth flux respectively.

The suitableborder linecircumstances for the speed, warmthplus concentrations fields are as follows,

$$t^{'}<0, u^{'}\left(y^{'}, t^{'}\right)=0, T^{'}=T_{\infty}^{'}, C^{'}=C_{\infty}^{'}$$

$$t^{'}\geq 0, u^{'}(y^{'}, t^{'})=U_0, T^{'}=T_w^{'}+\left(T_w^{'}-T_{\infty}^{'}\right)\varepsilon e^{i\omega^{'}t^{'}}, C^{'}=C_w^{'}+\left(C_w^{'}-C_{\infty}^{'}\right)\varepsilon e^{i\omega^{'}t^{'}}, at; y^{'}=0$$

$$u^{'}\left(y^{'}, t^{'}\right)=0, T^{'}=T_{\infty}^{'}, C^{'}=C_{\infty}^{'} as; y^{'}\to\infty \tag{13}$$

where $T^{'}$ the limited warmth of the Hydrophobic nanofluids and Q is the supplementary warmth basis. As opposed to that, β_f and β_c are the solid's and fluid's coefficients of thermal expansion, correspondingly, ρ_f and ρ_c are the parts of the fluid and solid that have different densities, correspondingly, whereas ρ_{nf} is the stickiness of the liquid nanoscale, α_{nf} is the thermal diffusivity of the fluid nanoparticles, and $(\rho C_p)_{nf}$ is the Capacitance of the fluid to warmth, radiative warmth flux q_r.

There is no self-absorption in the optically wide limit, but there is emission emitted by the limits that the liquid absorbs. According to Cogley's model $\frac{\partial q_r}{\partial y'}=4(T'-T_{\infty}')\int_0^{\infty}K_{\lambda w}\frac{de_{b\lambda}}{dT'}d\lambda=4I_1(T'-T_{\infty}')$.
The thickness, thermal diffusivity, warmth capacitance of the nan liquid is known by $\rho_{nf}=(1-\phi)\rho_f+\phi\rho_s, \left(\rho C_p\right)_{nf}=(1-\phi)\left(\rho C_p\right)_f+\phi\left(\rho C_p\right)_s, (\rho\beta)_{nf}=(1-\phi)(\rho\beta)_f+\phi(\rho\beta)_s$

The viscosity, thermal diffusivity, heat capacitance of the nanofluid is given by

$$\rho_{nf}=(1-\phi)\rho_f+\phi\rho_s\ , \left(\rho C_p\right)_{nf}=(1-\phi)\left(\rho C_p\right)_f+\phi\left(\rho C_p\right)_s\ , (\rho\beta)_{nf}=(1-\phi)(\rho\beta)_f+\phi(\rho\beta)_s$$
$$K_{nf}=K_f\left(\frac{K_s+2K_f-2\phi\left(K_f-K_s\right)}{K_s+2K_f+2\phi\left(K_f-K_s\right)}\right), \mu_{nf}=\frac{\mu_f}{(1-\phi)^{2.5}},\ \alpha_{nf}=\frac{K_{nf}}{\left(\rho C_p\right)_{nf}} \tag{14}$$

The Dimensionless variable is described in the following.

$$u=\frac{u^{'}}{U_0}, y=\frac{U_0 y^{'}}{\vartheta_f}, t=\frac{U_0^{\,2}t^{'}}{\vartheta_f}, \omega=\frac{\vartheta_f\omega^{'}}{U_0^{\,2}}, \theta=\frac{\left(T^{'}-T_{\infty}^{'}\right)}{\left(T_w^{'}-T_{\infty}^{'}\right)}, S=\frac{V_0}{U_0}, M=\frac{\sigma B_0^{\,2}\vartheta_f}{\rho_f U_0^{\,2}}, P_r=\frac{\vartheta_f}{\alpha_f}$$

$$D_u=\frac{D_m K_T\left(C_w^{'}-C_{\infty}^{'}\right)}{k_f C_s\left(T_w^{'}-T_{\infty}^{'}\right)}, Q_L=\frac{Q_l^{'}\left(C_w^{'}-C_{\infty}^{'}\right)}{U_0^{\,2}\left(T_w^{'}-T_{\infty}^{'}\right)}, K_r=\frac{K_l\vartheta_f}{U_0^{\,2}}, S_c=\frac{\vartheta_f}{D_B}, Q=\frac{Q^{'}\vartheta_f^{\,2}}{K_f U_0^{\,2}}$$

$$K=\frac{K'\rho_f U_0^2\vartheta_f^2}{\vartheta_f^2}\ ,\ G_r=\frac{(\rho\beta)_f\, g\vartheta_f(T_w'-T_{\infty}')}{\rho_f U_0^3},\ \varphi=\frac{(C'-C_{\infty}')}{(C_w'-C_{\infty}')},\ R=\frac{4I_1\vartheta_f^2}{k_f U_0^2} \tag{15}$$

Here

i. P_r is the Prandtlnumber,
ii. S is the suction parameter,

iii. M is Magnetic field parameter,
iv. K_r is the chemical reaction parameter,
v. S_c is the Schmidt number,
vi. G_r is theGrashof number,
vii. K is the Permeability parameter,
viii. D_u is the Diffusion thermo parameter,
ix. R is the Radiation parameter.

By means of non-dimensionless constraint quantities of Eq. (15), the equations Eq. (10) to Eq. (12) reduces to the subsequent non-dimensionless figure.

$$A\left(\frac{\partial u}{\partial t}-S\frac{\partial u}{\partial y}\right)=D\frac{\partial^2 u}{\partial y^2}+BG_1\theta-\left(M_1+\frac{D}{K}\right)u \tag{16}$$

Here $G_1=G_r\cos\gamma, M_1=m\sin\alpha^2$

$$C\left(\frac{\partial\theta}{\partial t}-S\frac{\partial\theta}{\partial y}-Q_L\varphi\right)=\frac{1}{P_r}\left(E\frac{\partial^2\theta}{\partial y^2}-F\theta+D_u\frac{\partial^2\varphi}{\partial y^2}\right) \tag{17}$$

where $F=Q+R$

$$\frac{\partial\varphi}{\partial t}-S\frac{\partial\varphi}{\partial y}=\frac{1}{S_c}\frac{\partial^2\varphi}{\partial y^2}-K_r\varphi \tag{18}$$

With the border linecircumstances

$$\begin{aligned}&t<0, u=0, \theta=0, \varphi=0\\ &t\geq 0, u=1, \theta=1+\varepsilon e^{i\omega t}, \varphi=1+\varepsilon e^{i\omega t} as, y=0\\ &u=0, \theta=0, \varphi=0 as, y\to\infty\end{aligned} \tag{19}$$

3. Solution of the Problem

Eq. (16) to Eq. (18) are Combined nonlinear the closed form solution of partial differential equations is possible. Though, analytically, it is possible to transform these equations into conventional differential equations. The main advantage of perturbation method is obtaining of the exact solution.We assume that velocity, temperature, withattention are expressed as follows:

$$u(y,t)=u_0+\varepsilon u_1 e^{i\omega t} \tag{20}$$

$$\theta(y,t)=\theta_0+\varepsilon\theta_1 e^{i\omega t} \tag{21}$$

$$\varphi(y,t) = \varphi_0 + \varepsilon\varphi_1 e^{i\omega t} \tag{22}$$

where ε << 1 is a parameter

Substituting Eq. (20) to Eq. (22) in equations Eq. (16) to Eq. (18) and equating zerothin addition to here are some ordinary differential equations based on first order equations.

$$Du''_0 + ASu'_0 - \left(M_1 + \frac{D}{K}\right)u_0 = -BG_1\theta_0 \tag{23}$$

$$Du''_1 + ASu'_1 - \left(\left(M_1 + \frac{D}{K}\right) + Ai\omega\right)u_1 = -BG_1\theta_1 \tag{24}$$

Here $G_1 = G_r\cos\gamma, M_1 = m\sin\alpha^2$

$$E\theta''_0 + P_rCS\theta'_0 - \mathrm{F}\,\theta_0 = -\,\mathrm{D_u}\varphi''_0 - \mathrm{P_r C\,Q_L}\varphi_0 \tag{25}$$

$$E\theta''_1 + P_rCS\theta'_1 - (\mathrm{FP_r Ci}\omega)\,\theta_1 = -\,\mathrm{D_u}\varphi''_1 - \mathrm{P_r C\,Q_L}\varphi_1 \tag{26}$$

$$\varphi''_0 + SS_c\varphi'_0 - K_rS_c\varphi_0 = 0 \tag{27}$$

$$\varphi''_1 + SS_c\varphi'_1 - (i\omega + K_r)S_c\varphi_1 = 0 \tag{28}$$

The boundary conditions Eq. (19) becomes

$$u_0 = 1; u_1 = 0; \theta_0 = 1, \theta_1 = 1, \varphi_0 = 1, \varphi_1 = 1, at; y = 0$$

$$u_0 = 0; u_1 = 0; \theta_0 = 0, \theta_1 = 0, \varphi_0 = 0, \varphi_1 = 0, as, y \to \infty \tag{29}$$

By substituting the border linecircumstances (Eq. (29)) in Eq. (27) to Eq. (28) we get

$$\begin{aligned}
u_0 &= B_5e^{-m_5y} + B_3e^{-m_3y} + B_4e^{-m_1y}\\
u_1 &= B_8e^{-m_6y} + B_6e^{-m_4y} + B_7e^{-m_2y}\\
\theta_0 &= B_1e^{-m_3y} + A_1e^{-m_1y}\\
\theta_1 &= B_2e^{-m_4y} + A_2e^{-m_2y}\\
\varphi_0 &= e^{-m_1y}\\
\varphi_1 &= e^{-m_2y}
\end{aligned} \tag{26}$$

Substituting the standards of equation Eq. (26) in equations Eq. (16) to Eq. (18), we get

$$u(y,t) = \left(B_5 e^{-m_5 y} + B_3 e^{-m_3 y} + B_4 e^{-m_1 y}\right) + \in \left(B_8 e^{-m_6 y} + B_6 e^{-m_4 y} + B_7 e^{-m_2 y}\right) e^{i\omega t} \tag{30}$$

$$\theta(y,t) = \left(B_1 e^{-m_3 y} + A_1 e^{-m_1 y}\right) + \in \left(B_2 e^{-m_4 y} + A_2 e^{-m_2 y}\right) e^{i\omega t} \tag{31}$$

$$\varphi(y,t) = \left(e^{-m_1 y}\right) + \in (e^{-m_2 y}) e^{i\omega t} \tag{32}$$

3.1 Shearing Stress

The shearing stress at the shieldin dimensional shape is given by

$$\tau = \left(\frac{\partial u}{\partial t}\right)_{y=0} = (-B_5 m_5 - B_3 m_3 - B_4 m_1) + \in \left(-B_8 m_6 - B_6 m_4 - B_7 m_2\right) e^{i\omega t} \tag{33}$$

3.2 Nusselt Number

The non- dimensional co-efficient of heat transfer defined by Nusseltnumber is given by

$$N_u = -\left(\frac{\partial \theta}{\partial t}\right)_{y=0} = (B_1 m_3 + A_1 m_1) + \in \left(B_2 m_4 + A_2 m_2\right) e^{i\omega t} \tag{34}$$

3.3 Sherwood Number

The non-dimensional co-efficient of mass transfer defined by Sherwood number is given by

$$S_h = -\left(\frac{\partial \varphi}{\partial t}\right)_{y=0} = m_1 + \in m_2 e^{i\omega t} \tag{35}$$

4. Result and Discussion

To highlight the key characteristics of the flow, The results are reported for the properties of heat and gathering transmission with fluid nanoparticles in Figure 2–16 and in Table 2 and 3. Numerical discussion is made of the impact of fluid nanoparticles on the distributions of speed, temperature, plusattentivenessin addition to on the coefficients of skin friction, heat transmission, and rate of heataccumulation. We have chosen, Sc=0.60, S=0.1, Kr=0.5, Q=2, K=4, M=0.5, QL=2, Gr=2, R=0.5, Du=2, α=π/6, γ=π/6, ϕ=0.05, $\varepsilon = 0.02, t = 1, \omega = 1$ *and* $\mathrm{Pr} = 0.71$

The additional variables, which are provided in figures, are varied over a range. Table 1 shows thermo physical properties of base fluid (Ethylene Glycol) and three different nano particles in S.I units.

Table 1
Thermo-physical properties of Ethylene Glycol and nanoparticles

Physical properties	$C_2H_6O_2$/Base fluid	Cu	CuO	TiO_2
ρ (kg/m^3)	1114	8933	3970	6500
c_p (J/kg K)	2415	385	765	540
k (w/m K)	0.25	401	40	18
β (1/K)	57 ×10^{-5}	1.67 ×10^{-5}	1.89 ×10^{-5}	0.85 ×10^{-5}

4.1 Magnetic Field Parameter's Impact (M)

Figure 2 demonstrates the common nanofluid velocity patterns for the nanoparticles. Cu, CuO and TiO_2 for varied the magnetic field's values constraint (M). It is clear from the graph that as the strength of the magnetic field rises, the fluid's nanofluid rapidity decreases. The Lorentz force is a resistive-type force that develops as the magnetic field's effect of a transverse effect on a liquid that conducts electricity. The border layer's fluid is prone to moving more slowly as a result of this force. Since the magnetic field retards these results numerically match assumptions for natural convection flow. In contrast to CuO-$C_2H_6O_2$ and TiO_2-$C_2H_6O_2$ nano liquid, the Lorentz force influence on Cu-$C_2H_6O_2$ nano liquid is the most significant. With a raise in the strength of the intriguing field, the outcome velocity is also reduced.

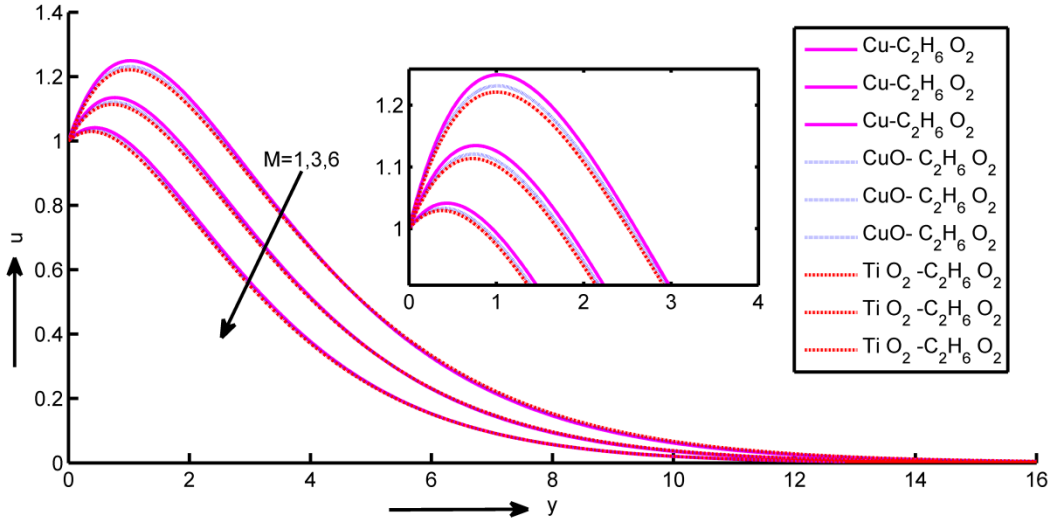

Fig. 2. Velocity profile for magnetic field parameter

4.2 Effect of Grashof Number (Gr)

Figure 3 demonstrates the result of Grashof number Gr on fluid velocity u for nanofluid $(\phi \neq 0)$. Figure's result shows that the fluid's velocity over the border linesheetraises by rising the values of Grashof number Gr for nanofluid with nanoparticles Cu, CuO and TiO_2. Additionally, it is noted that the highestspeed of the Cu-$C_2H_6O_2$ nanofluid is greater than that of the CuO-$C_2H_6O_2$ and TiO_2-$C_2H_6O_2$.

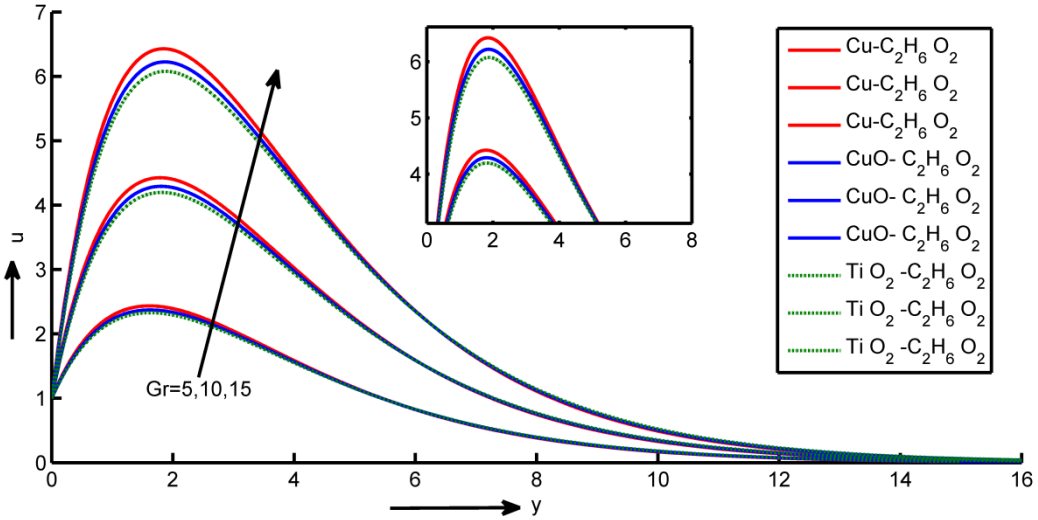

Fig. 3. Velocity profile for Grashof parameter

4.3 Effect of Heat Source Parameter (Q)

Figure 4 are graphical depiction of the temperature and velocity profiles at various values of Q with Cu, CuO and TiO_2 fluid nanoparticles. These numbers clearly show that when Q increases, the speed and hotness profiles also do. This is because an add to in heat generation or absorption specifications causes a reduce in the speed contours. Due to the hotness absorptions coefficient's dominance, it is stated that the velocity specifications velocity will decrease. It is also clear from Figure 11 that the heat will decrease when the heat source specification Q improves.

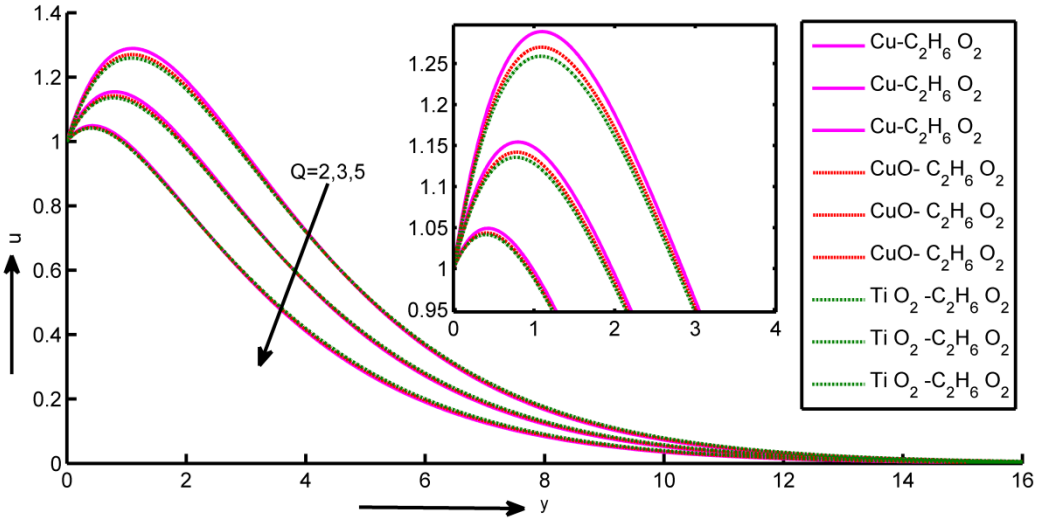

Fig. 4. Velocity profile for heat source parameter

4.4 Effect of Dufour Number (Du)

In Figure 5, it is depicted how the Diffusion-Thermo parameter (Du) affects the speed sharing of the Cu-$C_2H_6O_2$, CuO-$C_2H_6O_2$ and TiO_2-$C_2H_6O_2$ nanofluids, respectively. For both conventional and

nanofluids, it is observed that the border layer becomes thicker with Du. Thus, as the Dufour number rises, Additionally, the hydrodynamic border line sheet thickness.

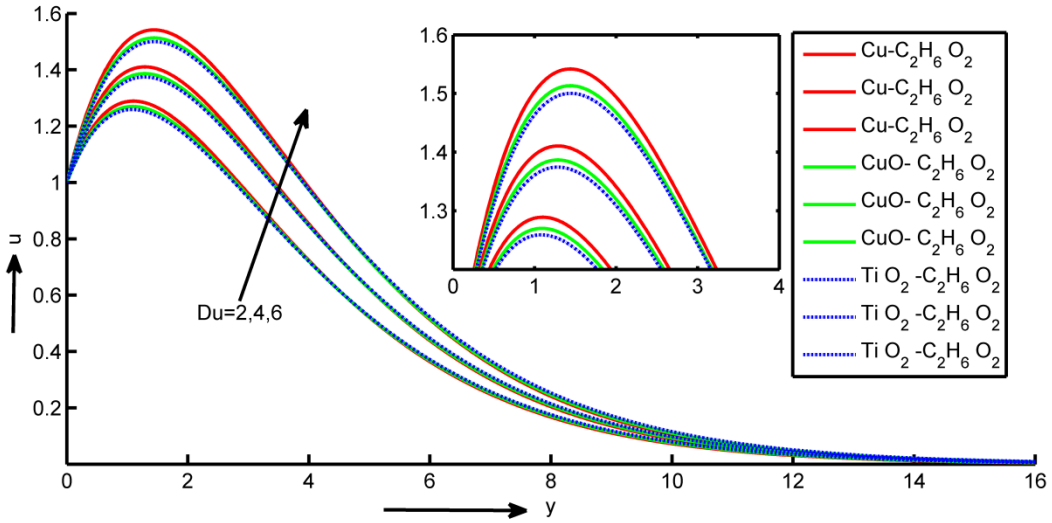

Fig. 5. Velocity profile for Dufour parameter

4.5 Effect of Permeability Parameter (K)

The Figure 6 depicted the impacts of permeability of the penetrable medium on velocity outlines of *u. The* magnitudes of the velocity constituents for improve with an enhancing in the penetrable specification *K*. The outcome velocity is also boost up with enhancing K for together Cu-$C_2H_6O_2$ as well as CuO-$C_2H_6O_2$ and TiO_2-$C_2H_6O_2$. Lesser the penetrability lowers the fluid velocity is noticed in the complete liquid regions.

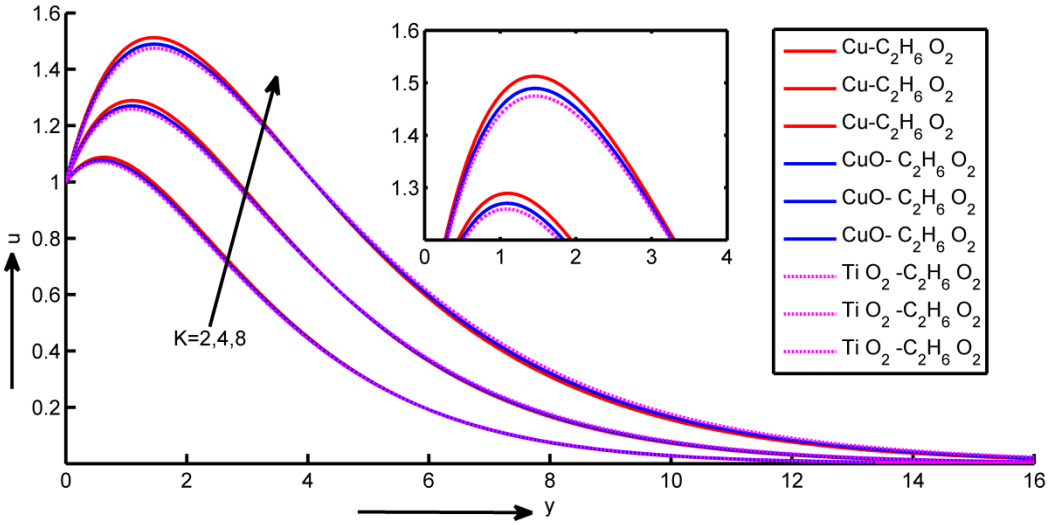

Fig. 6. Velocity profile for permeability parameter

4.6 Effect of Radiation Absorption Parameter (Q_L)

The heat and speed patterns for dissimilar principles of Q_L with Cu, CuO and TiO_2 nanoparticles are graphically represented in Figure 7. These figures amply demonstrate that the speed and

hotness profiles likewise enlarge when QL increases. This happens because the buoyancy force quickens the flood when heat is absorbed. Additionally, it's been discovered that the thermal boundary layer for Cu nanoparticles is significantly thicker than for CuO and TiO_2 nanoparticles. Large QL values are connected to a stronger predominance of radiation conduction over absorption, which results in thicker thermal and momentum border line layers and enhanced buoyant force.

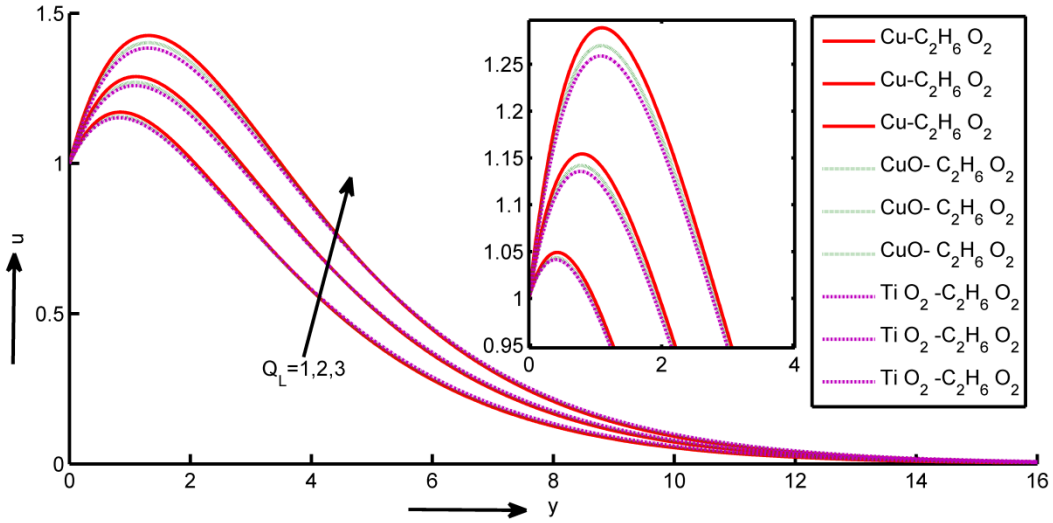

Fig. 7. Velocity profile for radiation absorption parameter

4.7 Effect of Suction Parameter (S)

Figure 8 demonstrates how fluid velocity u is affected by the suction parameter S for nanofluid $(\phi \neq 0)$. As an output of shape, it is evident that the fluid's cross-boundary sheet velocity decreases by increasing the suction constraint S for nanoparticle-containing nanofluid Cu, CuO and TiO_2. It is important to note that nanofluids with nanoparticles have a stronger result on the liquidspeed when the suction parameter S is present. Cu, CuO and TiO_2. Additionally, it is noted that Cu-$C_2H_6O_2$ nanofluid's maximum velocity is higher than that of the CuO-$C_2H_6O_2$ and TiO_2- $C_2H_6O_2$ nanofluid.

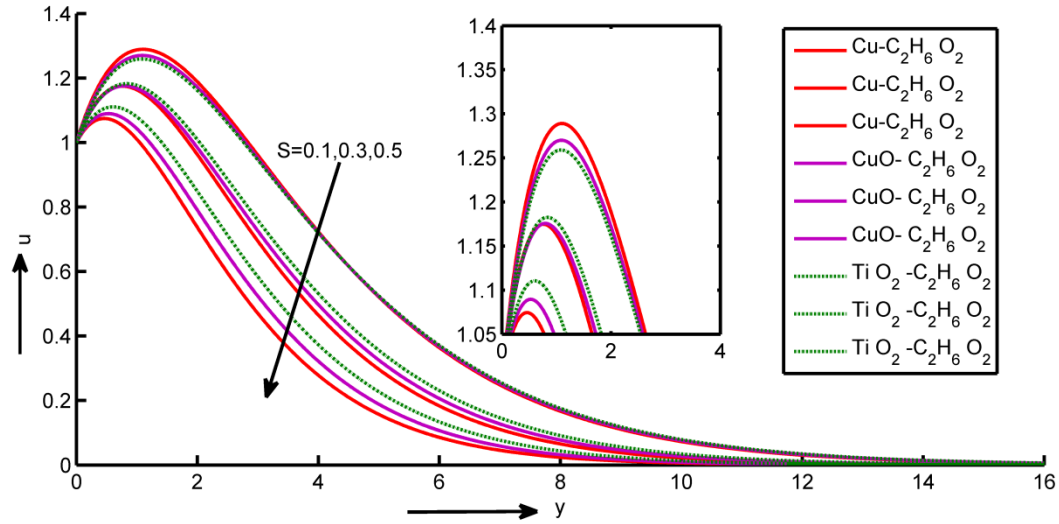

Fig. 8. Velocity profile for suction parameter

It is demonstrated how Du affects the heat profiles within the boundary layer in Figure 9. For Cu, CuO and TiO_2 nanofluids, it is seen that the hotness of the nanofluid raises with rising principles of Du, indicating that Du causes to increase the thickness of the thermal boundary layer. Additionally, at lower values of the Dufour number for both conventional fluids and nanofluids, the thermal border linesheet shrinks extraspeedily. Physically, lessening Due to Du, species gradients have a noticeably smaller effect on the temperature field, which leads to noticeably minorhotness function values and a cooling of the border line sheet regime. Alternatively, the concentration function in the boundary layer regime rises as Du decreases. The contribution of hotness gradients obviouslymodifiedaccumulation diffusion in the domain.

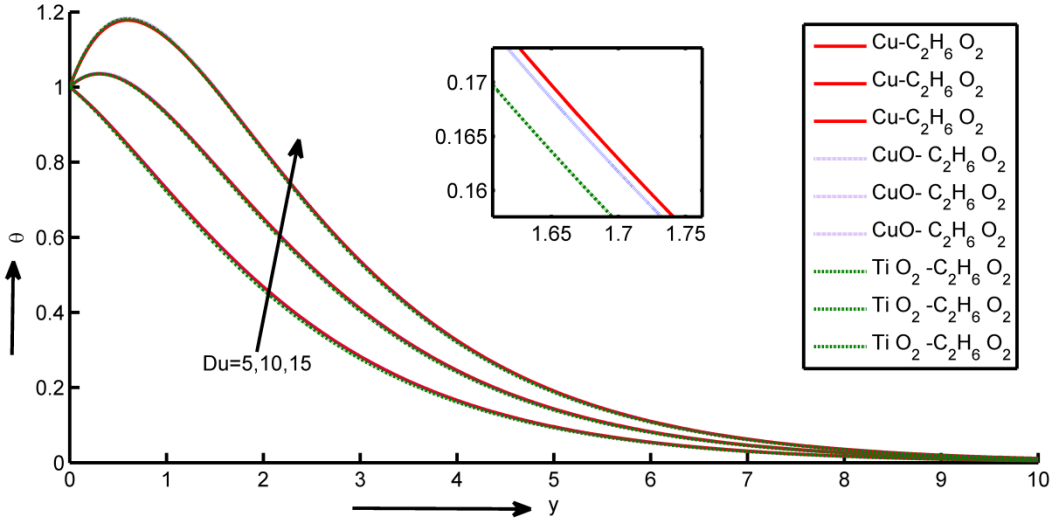

Fig. 9. Temperature profile for Dufour parameter

Figure 10 illustration of radiation's influence on temperature silhouettes. Radiation specifications improve flow temperature profiles when increased. Physically, increasing radiation warms the flow and increases the thickness of the thermally boundary stratums.

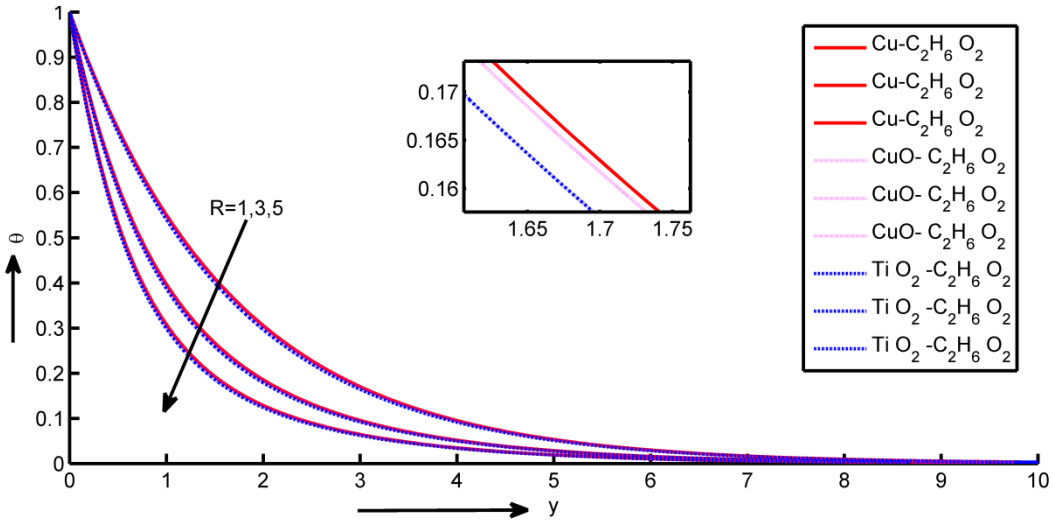

Fig. 10. Temperature profile for radiation parameter

Figure 11 are graphical depiction of the temperature and velocity profiles at various values of Q with Cu, CuO and TiO_2 fluid nanoparticles. These numbers clearly show that when Q increases, the

speed and hotness profiles also do. This is because an add to in heat generation or absorption specifications causes a reduce in the speed contours. Due to the hotness absorptions coefficient's dominance, it is stated that the velocity specifications velocity will decrease. It is also clear from Figure 11 that the heat will decrease when the heat source specification Q improves.

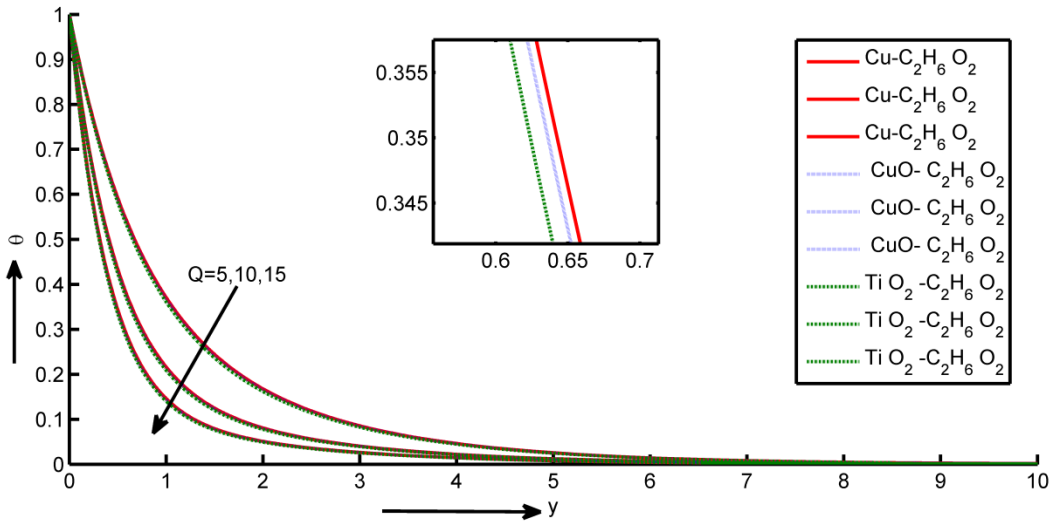

Fig. 11. Temperature profile for heat source parameter

Figure 12 shows that temperature enhances with raising the values of Prandtl number. It's observed that maximum temperature of CuO-$C_2H_6O_2$Nanofluid is superior to that of theCu- $C_2H_6O_2$, TiO_2- $C_2H_6O_2$nanofluid.

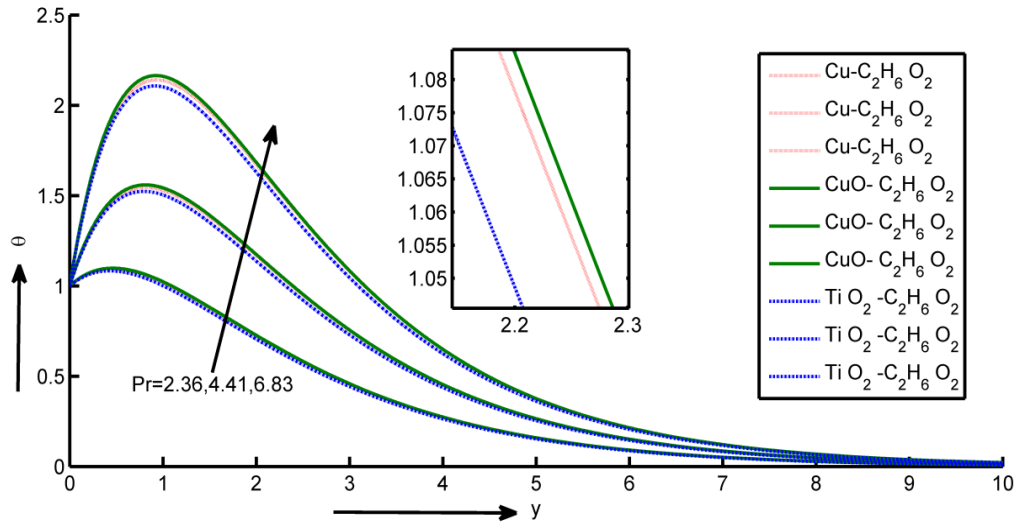

Fig. 12. Temperature profile for Prandtl number

The heat and speed patterns for dissimilarprinciples of Q_L with Cu, CuO andTiO_2nanoparticles are graphically represented in Figure 13. These figures amply demonstrate that the speed and hotness profiles likewise enlarge when QL increases. This happens because the buoyancy force quickens the flood when heat is absorbed.Additionally, it's been discovered that the thermal boundary layer for Cu nanoparticles is significantly thicker than for CuO andTiO_2nanoparticles. Large QL values are connected to a stronger predominance of radiation conduction over

absorption, which results in thicker thermal and momentum border line layers and enhanced buoyant force.

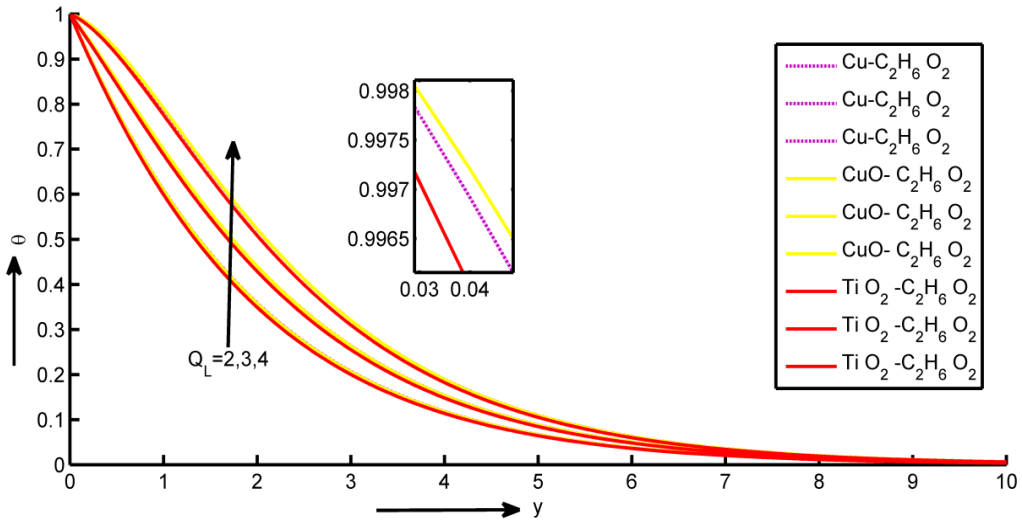

Fig. 13. Temperature profile for radiation absorption parameter

4.8 Effect of Schmidt Number (Sc)

Figure 14 depicts the modification of the flow field's attentivenessborder linesheetfor H_2, He, H_2O vapor, and NH_3. This figure displays the concentration distribution in the presence of the flow field. It is clear from comparing the curves in the aforementioned picture that the flow field's concentration border linecoating thickness decreases at every location as the Schmidt number rises. As a result, the attentiveness buoyant effects are lessened, which lowers fluid flow. Along with the lowering of the attentiveness profiles, the border sheet of concentration also falls.

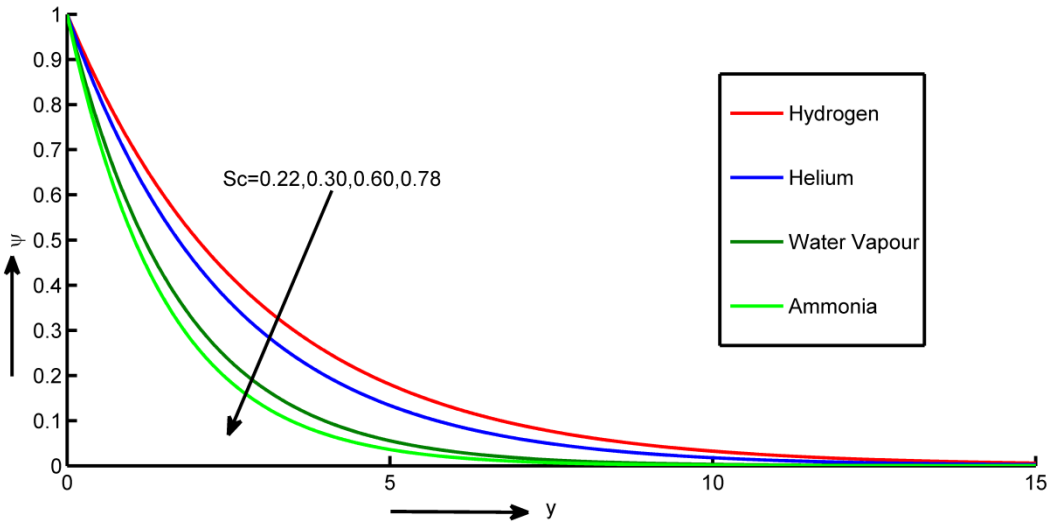

Fig. 14. Profile of concentration for the Schmidt number

4.9 Chemical Reaction Parameter Effect (Kr)

The patterns of attention for dissimilar levels of the harmful substance response restrictionKr (>0) are given in Figure 15. The fluid's concentration will be reduced by an increase in the substanceresponsestricture. Less diffusion results from higher concentrations of Kr, which cause the chemical molecule diffusivity to decrease. They were therefore created by a species transfer. A rise in Kr will suppress the concentration of species. The concentration distribution decreases everywhere in the flow field when the reaction parameter is increased.

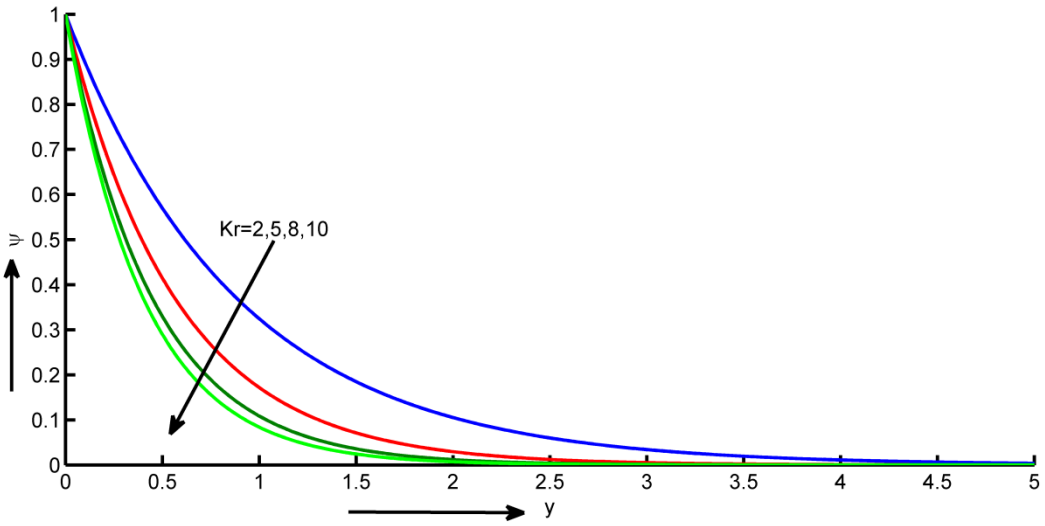

Fig. 15. Concentration profile for chemical reaction parameter

The effects of the suction parameter (S) on it displays the species concentration profiles. in Figure 16. The solutal border linesheet thickness reduces as the suction parameter raises the species concentration. This is because the suction often stabilizes border growth. From a physical perspective, these effects are undoubtedly substantiated.

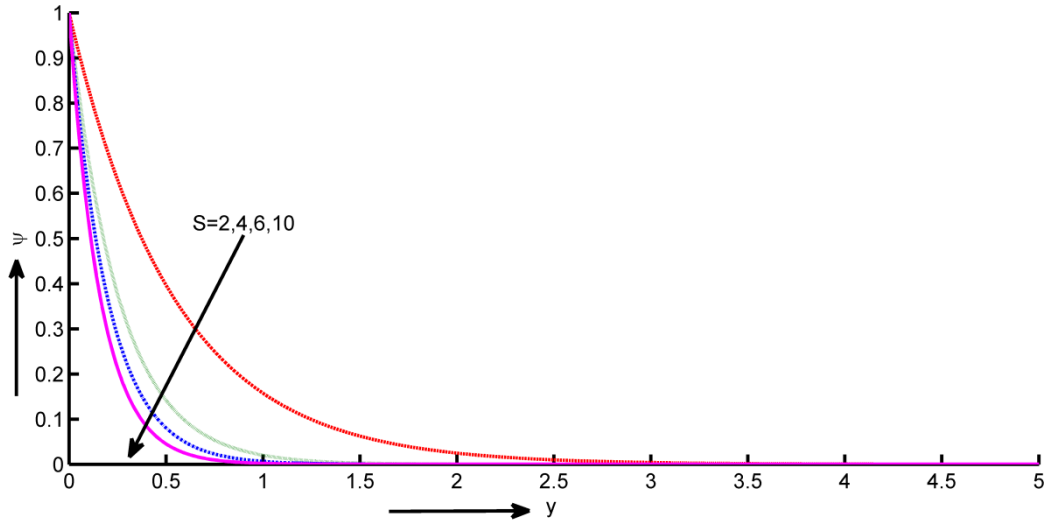

Fig. 16. Concentration profile for suction parameter

The variations in skin friction under the influence of significant parameters are clearly shown in Table 2 for three types of nanofluids.

Table 2

Skin friction

Gr	M	K	Q_L	Du	Kr	ϕ	α	Γ	Skin friction(τ)		
									$Cu\text{-}C_2H_6O_2$	$TiO_2\text{-}C_2H_6O_2$	$CuO\text{-}C_2H_6O_2$
1									0.5210	0.2456	-0.2456
2									0.8452	0.6452	-0.1045
3									1.6592	1.4564	0.1366
	0.1								1.2345	1.2866	0.0386
	0.5								0.8567	0.8546	-0.1543
	1.0								0.6542	0.5234	-0.3164
		2							0.6421	0.5920	-0.3682
		4							0.8543	0.8436	-0.2065
		6							1.1845	1.2456	-0.0465
			1						0.7892	0.8651	-0.1723
			3						1.3497	1.4723	-0.0672
			5						1.5943	1.7795	0.0684
				0.1					0.7368	0.6864	-0.1434
				0.2					0.7489	0.6998	-0.1385
				0.3					0.7548	0.7045	-0.1358
					3				0.9043	0.8358	-0.1534
					5				0.9345	0.9978	-0.1555
					9				0.9864	1.2926	-0.1566
						0.05			0.8275	0.9768	-0.0145
						0.15			0.7668	0.6843	-0.0832
						0.25			0.5120	0.4465	-0.1255
							π/12		1.3152	1.1729	0.0639
							π/6		0.9875	0.9766	-0.0301
							π/4		0.8638	0.7728	-0.1166
								π/12	1.1870	1.1564	0.4115
								π/6	0.9475	0.9227	0.3218
								π/4	0.7518	0.6945	0.1792

Also, the changes in Nusselt number are depicted in Table 3 for three types of nanofluids.

Table 3
Nusselt number

S	Du	ϕ	Q_L	Q			
					$Cu\text{-}C_2H_6O_2$	$CuO\text{-}C_2H_6O_2$	$Tio_2\text{-}C_2H_6O_2$
0.2					0.2407	0.2369	0.2467
0.5					0.2190	0.2147	0.2220
1.2					0.1485	0.1428	0.1427
	0.2				0.2468	0.7112	0.7307
	0.3				-0.0083	0.6852	0.7042
	0.4				-0.2635	0.6592	0.6777
		0.06			0.1805	0.1786	0.1832
		0.18			0.2399	0.2363	0.2463
		0.3			0.2679	0.2653	0.2770
			3		0.0949	0.0876	0.1017
			5		-0.2088	-0.2236	-0.2021
			7		-0.5126	-0.5347	-0.5060
				4	0.7207	0.7246	0.7408
				5	0.9079	0.9147	0.9330
				6	1.0751	1.0844	1.1047

5. Conclusions

The study's findings with the novelty of including thermal radiation and angle of inclination can be stated as the following deductions:

i. As far as nanoparticles are concernedCu, CuO andTiO_2, with an increasing heat source parameter, magnetic field restriction, and suction restriction, boundary layer fluid velocity decreases, while it increases with agrowing Grashof number, Dufour digit, permeability parameterand radiation absorption constraint.
ii. As the Dufour number rises, the thermal border linecoating thickness increases, radiation absorption parameterand Prandtl number rise.
iii. A decrease in species concentration occurs with a rise in the suction constraint, the substanceresponseconstraintand the Schmidt number.
iv. Skin friction coefficient is significantly affected by M and QL.

Acknowledgement
This research was not funded by any grant.

References

[1] Ali, Abu Raihan Ibna, and Bodius Salam. "A review on nanofluid: preparation, stability, thermophysical properties, heat transfer characteristics and application." *SN Applied Sciences* 2, no. 10 (2020): 1636.https://doi.org/10.1007/s42452-020-03427-1
[2] Eastman, Jeffrey A., S. U. S. Choi, Sheng Li, W. Yu, and L. J. Thompson. "Anomalously increased effective thermal conductivities of ethylene glycol-based nanofluids containing copper nanoparticles." *Applied physics letters* 78, no. 6 (2001): 718-720.https://doi.org/10.1063/1.1341218
[3] Hamilton, R. L, and O. K. Crosser. "Thermal conductivity of heterogeneous two-component systems." *Industrial & Engineering chemistry fundamentals* 1, no. 3 (1962): 187-191.https://doi.org/10.1021/i160003a005
[4] Sharma, Prabhakar, Zafar Said, Anurag Kumar, Sandro Nizetic, Ashok Pandey, Anh Tuan Hoang, Zuohua Huang *et al.,* "Recent advances in machine learning research for nanofluid-based heat transfer in renewable energy system." *Energy & Fuels* 36, no. 13 (2022): 6626-6658.https://doi.org/10.1021/acs.energyfuels.2c01006
[5] Jama, Mohamoud, Tejvir Singh, Seifelislam Mahmoud Gamaleldin, Muammer Koc, Ayman Samara, Rima J. Isaifan, and Muataz A. Atieh. "Critical review on nanofluids: preparation, characterization, and applications." *Journal of Nanomaterials* 2016 (2016).https://doi.org/10.1155/2016/6717624
[6] Kleinstreuer, Clement, and Yu Feng. "Experimental and theoretical studies of nanofluid thermal conductivity enhancement: a review." *Nanoscale research letters* 6 (2011): 1-13.https://doi.org/10.1186/1556-276X-6-229
[7] Li, Junhao, Xilong Zhang, Bin Xu, and Mingyu Yuan. "Nanofluid research and applications: A review." *International Communications in Heat and Mass Transfer* 127 (2021): 105543.https://doi.org/10.1016/j.icheatmasstransfer.2021.105543
[8] Wahid, Nur Syahirah, Norihan Md Arifin, Najiyah Safwa Khashi'ie, Ioan Pop, Norfifah Bachok, and Mohd Ezad Hafidz Hafidzuddin. "Hybrid nanofluid stagnation point flow past a slip shrinking Riga plate." *Chinese Journal of Physics* 78 (2022): 180-193.https://doi.org/10.1016/j.cjph.2022.05.016
[9] Malvandi, A., F. Hedayati, and D. D. Ganji. "Nanofluid flow on the stagnation point of a permeable non-linearly stretching/shrinking sheet." *Alexandria engineering journal* 57, no. 4 (2018): 2199-2208.https://doi.org/10.1016/j.aej.2017.08.010
[10] Bhattacharyya, Krishnendu, Swati Mukhopadhyay, and G. C. Layek. "Slip effects on boundary layer stagnation-point flow and heat transfer towards a shrinking sheet." *International Journal of Heat and Mass Transfer* 54, no. 1-3 (2011): 308-313.https://doi.org/10.1016/j.ijheatmasstransfer.2010.09.041
[11] Aly, Emad H., and I. Pop. "MHD flow and heat transfer near stagnation point over a stretching/shrinking surface with partial slip and viscous dissipation: Hybrid nanofluid versus nanofluid." *Powder Technology* 367 (2020): 192-205.https://doi.org/10.1016/j.powtec.2020.03.030
[12] Salehi, Sajad, Amin Nori, Kh Hosseinzadeh, and D. D. Ganji. "Hydrothermal analysis of MHD squeezing mixture fluid suspended by hybrid nanoparticles between two parallel plates." *Case Studies in Thermal Engineering* 21 (2020): 100650.https://doi.org/10.1016/j.csite.2020.100650

[13] Manohar, G. R., P. Venkatesh, B. J. Gireesha, J. K. Madhukesh, and G. K. Ramesh. "Performance of water, ethylene glycol, engine oil conveying SWCNT-MWCNT nanoparticles over a cylindrical fin subject to magnetic field and heat generation." *International Journal of Modelling and Simulation* 42, no. 6 (2022): 936-945.https://doi.org/10.1080/02286203.2021.2004296

[14] Madhukesh, Javali K., Gosikere K. Ramesh, Govinakovi S. Roopa, Ballajja C. Prasannakumara, Nehad Ali Shah, and Se-Jin Yook. "3D flow of hybrid nanomaterial through a circular cylinder: Saddle and Nodal Point Aspects." *Mathematics* 10, no. 7 (2022): 1185.https://doi.org/10.3390/math10071185

[15] Ismoen, Muhaimin, Radiah Bte Mohamad, R. Kandasamy, Suliadi Firdaus Sufahani, Fazlul Karim, and Muhamad Sabirin. "Numerical Investigation for Convective Heat Transfer of CNT Nano-Fluids over a Stretching Surface." In *Materials Science Forum*, vol. 961, pp. 148-155. Trans Tech Publications Ltd, 2019.https://doi.org/10.4028/www.scientific.net/MSF.961.148

[16] Das, S., S. K. Guchhait, and R. N. Jana. "Effects of Hall currents and radiation on unsteady MHD flow past a heated moving vertical plate." *Journal of Applied Fluid Mechanics* 7, no. 4 (2014): 683-692.https://doi.org/10.36884/jafm.7.04.21486

[17] Balla, Chandra Shekar, Naikoti Kishan, Rama SR Gorla, and B. J. Gireesha. "MHD boundary layer flow and heat transfer in an inclined porous square cavity filled with nanofluids." *Ain Shams Engineering Journal* 8, no. 2 (2017): 237-254.https://doi.org/10.1016/j.asej.2016.02.010

[18] Adnan, Umar Khan, Naveed Ahmed, Syed Tauseef Mohyud-Din, M. D. Alsulami, and Ilyas Khan. "A novel analysis of heat transfer in the nanofluid composed by nanodimaond and silver nanomaterials: numerical investigation." *Scientific Reports* 12, no. 1 (2022): 1284.https://doi.org/10.1038/s41598-021-04658-x

[19] Archit, Dave, Sharma Kuldeep, and Chandramuly R. Sharma. "Comprehensive study on graphene nanofluids and its applications: Literature review." *Research Journal of Science and Technology* 13, no. 3 (2021): 200-204.https://doi.org/10.52711/2349-2988.2021.00030

[20] Choi, S. US, and Jeffrey A. Eastman. *Enhancing thermal conductivity of fluids with nanoparticles*. No. ANL/MSD/CP-84938; CONF-951135-29. Argonne National Lab.(ANL), Argonne, IL (United States), 1995.

[21] Krishna, M. Veera, N. Ameer Ahammad, and Ali J. Chamkha. "Radiative MHD flow of Casson hybrid nanofluid over an infinite exponentially accelerated vertical porous surface." *Case Studies in Thermal Engineering* 27 (2021): 101229.https://doi.org/10.1016/j.csite.2021.101229

[22] Hayat, Tasawar, Anum Nassem, Muhammad Ijaz Khan, Muhammad Farooq, and Ahmed Al-Saedi. "Magnetohydrodynamic (MHD) flow of nanofluid with double stratification and slip conditions." *Physics and Chemistry of Liquids* 56, no. 2 (2018): 189-208.https://doi.org/10.1080/00319104.2017.1317778

[23] Khan, Umar, Naveed Ahmed, and Syed Tauseef Mohyud-Din. "Heat transfer enhancement in hydromagnetic dissipative flow past a moving wedge suspended by H2O-aluminum alloy nanoparticles in the presence of thermal radiation." *International Journal of Hydrogen Energy* 42, no. 39 (2017): 24634-24644.https://doi.org/10.1016/j.ijhydene.2017.07.127

[24] Hayat, Tasawar, Sumaira Qayyum, Maria Imtiaz, and Ahmed Alsaedi. "Comparative study of silver and copper water nanofluids with mixed convection and nonlinear thermal radiation." *International Journal of Heat and Mass Transfer* 102 (2016): 723-732.https://doi.org/10.1016/j.ijheatmasstransfer.2016.06.059

[25] Sheikholeslami, Mohsen, and Mohadeseh Seyednezhad. "Simulation of nanofluid flow and natural convection in a porous media under the influence of electric field using CVFEM." *International Journal of Heat and Mass Transfer* 120 (2018): 772-781.https://doi.org/10.1016/j.ijheatmasstransfer.2017.12.087

[26] Kodi, Raghunath, Obulesu Mopuri, Sujatha Sree, and Venkateswaraju Konduru. "Investigation of MHD Casson fluid flow past a vertical porous plate under the influence of thermal diffusion and chemical reaction." *Heat Transfer* 51, no. 1 (2022): 377-394.https://doi.org/10.1002/htj.22311

[27] Kumar, RVMSS Kiran, P. Durga Prasad, and S. V. K. Varma. "Analytical study of heat and mass transfer enhancement in free convection flow with chemical reaction and constant heat source in nanofluids." *Procedia Engineering* 127 (2015): 978-985.https://doi.org/10.1016/j.proeng.2015.11.446

[28] Kumar, RVMSS Kiran, P. Durga Prasad, and S. V. K. Varma. "Thermo-diffusion and chemical reaction effects on free convective heat and mass transfer flow of conducting nanofluid through porous medium in a rotating frame." *Global Journal of Pure and Applied Mathematics (GJPAM)* 12, no. 1 (2016): 2016.

[29] Eckert, E. RG, and Robert M. Drake Jr. "Analysis of heat and mass transfer." (1987).

[30] Basant Kumar, J. H. A., and A. K. Singh. "Soret effects on free-convection and mass transfer flow in the stokes problem for a infinite vertical plate." *Astrophysics and Space Science* 173 (1990): 251-255.https://doi.org/10.1007/BF00643934

[31] Prasad, P. Durga, RVMSS Kiran Kumar, and S. V. K. Varma. "Heat and mass transfer analysis for the MHD flow of nanofluid with radiation absorption." *Ain Shams Engineering Journal* 9, no. 4 (2018): 801-813.https://doi.org/10.1016/j.asej.2016.04.016

[32] Zeeshan, Ahmed, Muhammad Awais, Faris Alzahrani, and Nasir Shehzad. "Energy analysis of non-Newtonian nanofluid flow over parabola of revolution on the horizontal surface with catalytic chemical reaction." *Heat Transfer* 50, no. 6 (2021): 6189-6209.https://doi.org/10.1002/htj.22168
[33] Salahuddin, T., Muhammad Awais, and Wei-Feng Xia. "Variable thermo-physical characteristics of Carreau fluid flow by means of stretchable paraboloid surface with activation energy and heat generation." *Case Studies in Thermal Engineering* 25 (2021): 100971.https://doi.org/10.1016/j.csite.2021.100971
[34] Salahuddin, T., and Muhammad Awais. "A comparative study of Cross and Carreau fluid models having variable fluid characteristics." *International Communications in Heat and Mass Transfer* 139 (2022): 106431.https://doi.org/10.1016/j.icheatmasstransfer.2022.106431
[35] Salahuddin, T., Aaqib Javed, Mair Khan, M. Awais, and Harun Bangali. "The impact of Soret and Dufour on permeable flow analysis of Carreau fluid near thermally radiated cylinder." *International Communications in Heat and Mass Transfer* 138 (2022): 106378.https://doi.org/10.1016/j.icheatmasstransfer.2022.106378
[36] Salahuddin, T., Zoehib Mahmood, Mair Khan, and Muhammad Awais. "A permeable squeezed flow analysis of Maxwell fluid near a sensor surface with radiation and chemical reaction." *Chemical Physics* 562 (2022): 111627.https://doi.org/10.1016/j.chemphys.2022.111627
[37] Salahuddin, T., Mair Khan, and Muhammad Awais. "A noteworthy impact of heat and mass transpiration near the unsteady rare stagnation region." *Pramana* 96, no. 1 (2022): 48.https://doi.org/10.1007/s12043-021-02283-x
[38] Salahuddin, T., Z. Ali, Muhammad Awais, Mair Khan, and Mohamed Altanji. "A flow behavior of Sutterby nanofluid near the catalytic parabolic surface." *International Communications in Heat and Mass Transfer* 131 (2022): 105821.https://doi.org/10.1016/j.icheatmasstransfer.2021.105821
[39] Salahuddin, T., Muhammad Awais, Mair Khan, and Mohamed Altanji. "Analysis of transport phenomenon in cross fluid using Cattaneo-Christov theory for heat and mass fluxes with variable viscosity." *International Communications in Heat and Mass Transfer* 129 (2021): 105664.https://doi.org/10.1016/j.icheatmasstransfer.2021.105664